PHYSICAL REVIEW C VOLUME 22, NUMBER 2 AUGUST 1980

Three-dimensional charge dispersion curves from interactions of 11–29 GeV protons with uranium

Yu-Wen Yu
Institute of Nuclear Science, National Tsing Hua University, Hsing-Chu, Taiwan, Republic of China
(Received 8 March 1979)

Experimental nuclear charge-dispersion curves from interactions of 11–29 GeV protons with ^{238}U have been used in the construction of three-dimensional charge-dispersion curves. They show the yield variation with mass number A. Neutron-deficient products are distributed over the entire mass range with a peak at A near 87, while the yield of neutron-excessive products is distributed only in the relatively narrow mass region between $A = 70$ and $A = 150$ and has a maximum around $A = 115$. An isobaric yield curve has been obtained by summing up each of the charge-dispersion curves and shows a peak, rather than the flat top, in the mass region $A = 80$ to 140 reported previously. The mass yield curves of neutron-excessive and neutron-deficient products are obtained by a decomposition of the charge-dispersion curve with two Gaussians, and the mechanism of formation is suggested.

[NUCLEAR REACTIONS High energy proton-induced nuclear fission, fragmentation, spallation, isobaric yield and three-dimensional charge dispersion curves.]

Since the double humped isobaric charge-dispersion yield from interaction of ^{238}U with GeV protons has been observed near $A = 130$,[1] this indicates that at least two different mechanisms could be involved in such a reaction. One is characterized by low deposition energy yields of neutron-excessive products known from binary fission processes. The other is characterized by high deposition energy from a fast break process and, following evaporation of neutrons, yields neutron-deficient products. This process is believed to occur from fragmentation rather than spallation.[2] These two distinct mechanisms have been confirmed by recoil range experiments.[3] Recently Chu *et al.*[4,5] showed that the charge-dispersion curves (CDC) for light and heavy isobars at $A = 45$ and $A = 170$, respectively, have only single peaks. Therefore it is quite interesting to find how the two mechanisms contribute to each isobaric charge dispersion yield and how they vary with A.

In the last several years, a number of isobaric charge dispersion curves have been reported for

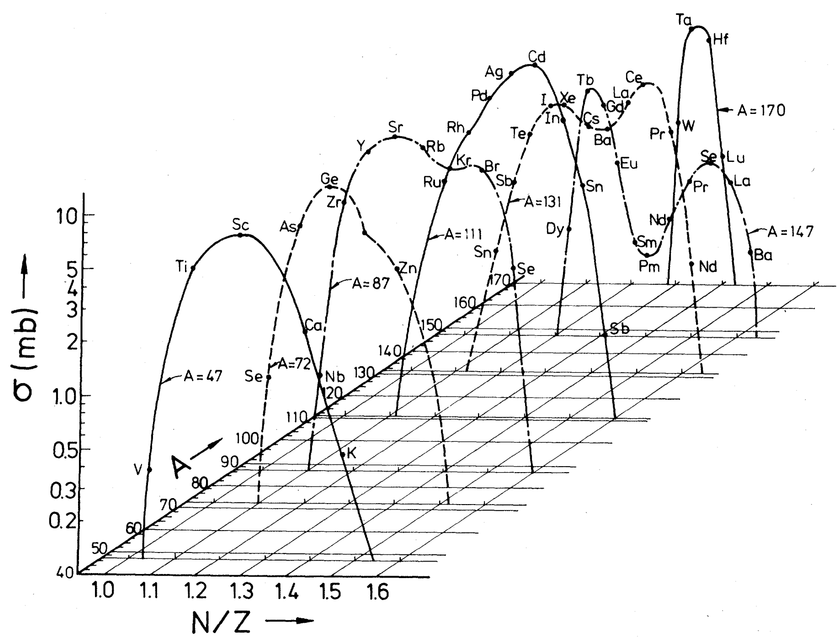

FIG. 1. Three-dimensional charge-dispersion curves of interaction of uranium with 11–29 GeV protons.

TABLE I. Summary of cross sections from reported CDC's.

Nuclide	N/Z	σ (mb)	Nuclide	N/Z	σ (mb)
$^{47}_{19}K$	1.474	0.39	$^{131}_{50}Sn$	1.620	0.4
$^{47}_{20}Ca$	1.350	1.8	$^{131}_{51}Sb$	1.569	2.1
$^{47}_{21}Sc$	1.238	6.3	$^{131}_{52}Te$	1.519	4.0
$^{47}_{22}Ti$	1.136	4.1	$^{131}_{53}I$	1.472	3.1
$^{47}_{23}V$	1.043	0.31	$^{131}_{54}Xe$	1.426	2.2
$^{72}_{30}Zn$	1.400	1.3	$^{131}_{55}Cs$	1.382	2.3
$^{72}_{31}Ga$	1.323	3.2	$^{131}_{56}Ba$	1.339	2.9
$^{72}_{32}Ge$	1.250	5.8	$^{131}_{57}La$	1.298	3.0
$^{72}_{33}As$	1.182	3.4	$^{131}_{58}Ce$	1.259	2.0
$^{72}_{34}Se$	1.118	0.5	$^{131}_{59}Pr$	1.220	1.1
$^{87}_{34}Se$	1.559	1.2	$^{147}_{56}Ba$	1.625	0.30
$^{87}_{35}Br$	1.486	4.7	$^{147}_{57}La$	1.579	0.74
$^{87}_{36}Kr$	1.417	4.6	$^{147}_{58}Ce$	1.534	0.93
$^{87}_{37}Rb$	1.351	6.1	$^{147}_{59}Pr$	1.492	0.72
$^{87}_{38}Sr$	1.289	7.2	$^{147}_{60}Nd$	1.450	0.45
$^{87}_{39}Y$	1.231	5.7	$^{147}_{61}Pm$	1.410	0.28
$^{87}_{40}Zr$	1.175	3.2	$^{147}_{62}Sm$	1.371	0.33
$^{87}_{41}Nb$	1.122	0.34	$^{147}_{63}Eu$	1.333	0.91
$^{111}_{43}Tc$	1.581	0.28	$^{147}_{64}Gd$	1.297	1.9
$^{111}_{44}Ru$	1.523	1.9	$^{147}_{65}Tb$	1.262	2.3
$^{111}_{45}Rh$	1.467	5.4	$^{147}_{66}Dy$	1.227	0.39
$^{111}_{46}Pd$	1.413	9.0	$^{170}_{70}Yb$	1.428	0.072
$^{111}_{47}Ag$	1.362	7.9	$^{170}_{71}Lu$	1.394	0.52
$^{111}_{48}Cd$	1.313	4.8	$^{170}_{72}Hf$	1.361	2.3
$^{111}_{49}In$	1.265	3.7	$^{170}_{73}Ta$	1.329	2.7
$^{111}_{50}Sn$	1.220	2.0	$^{170}_{74}W$	1.297	0.78
$^{111}_{51}Sb$	1.176	0.5	$^{170}_{75}Re$	1.267	0.038

the interaction of ^{238}U with protons of energies in the region 11.5 to 29 GeV. They are $A=45$ measured by Chu *et al.*[4] at 28.5 GeV; $A=74$ determined by Kaufman[6] at 18 GeV, $A=111$ by Panontin and Porile[7] at 11.5 GeV, $A=131$ by Yu and Porile[3] at 11.5 GeV, $A=147$ and $A=170$ by Chu *et al.*[5] at 28 GeV, plus the CDC at $A=87$ obtained from transformation of the isotopic yield distribution of Rb isotopes measured by Chanmont[8] at 24 GeV to the CDC with the method described in Ref. 3, a total of seven known CDC. At proton energies greater than 10 GeV the yield is essentially independent of bombarding energy.[9,10] Therefore these CD curves allow us to construct a three-dimensional charge-dispersion curve by plotting the yield versus A and N/Z. From it one can see the variation with A of the products from the two mechanisms in a CDC.

TABLE II. Isobaric cross sections for the interaction of 11–29 GeV protons with uranium.

Mass number	Isobaric yield (mb)	Reference
47	12.9	Ref. 4
72	15.5	Ref. 6
87	32.3	Ref. 8
111	35.0	Ref. 7
131	23.4	Ref. 3
147	9.1	Ref. 5
170	5.1	Ref. 5

In the construction of the three-dimensional CD curves, we first have to unify the abscissa from Z_{eff}-Z, Z_A-Z, and Z_p-Z to N/Z. The reason we choose N/Z instead of Z_A-Z is because these CD curves cover a large range of A. We avoid the discontinuity of the shells, and using the N/Z as abscissa shows better agreement with experimental data through transformations.[3] Therefore we use it together with the yields that are taken from reported CD curves, rather than individual experiments. The results are given in Table I and presented in Fig. 1. Summing up each CDC gives an isobaric yield of A which we list in Table II and plot in Fig. 2.

Figure 1 contains the three dimensional charge-dispersion curves. From it we can see that the neutron-excessive products start to contribute at A around 70 and reach a maximum at $A=111$, then fall away at $A=170$, forming a Gaussianlike peak along the A axis. The distribution of neutron-excessive products is much like that from the interaction of low-energy protons with ^{238}U which has been confirmed as a binary fission process by the mica-track technique[11] and by recoil range measurements.[3] On the other hand, the neutron-deficient products observed from light to heavy nuclides cover the entire range of A. According to general trends of spallation, one expects the yields to drop or, at most, stay constant with decreasing mass number A. Both the BNL group[5] and the Chicago group[10] believe that a flat distribution of spallation yield over the entire range of A is to be expected, but from Fig. 1 we can see that the distribution of the neutron-deficient yields does not confirm this. They are distributed over the entire mass region but also form a peak with maximum around $A=90$. This distribution cannot be interpreted by either the mechanism of spallation or of fission. From recoil range measurements and

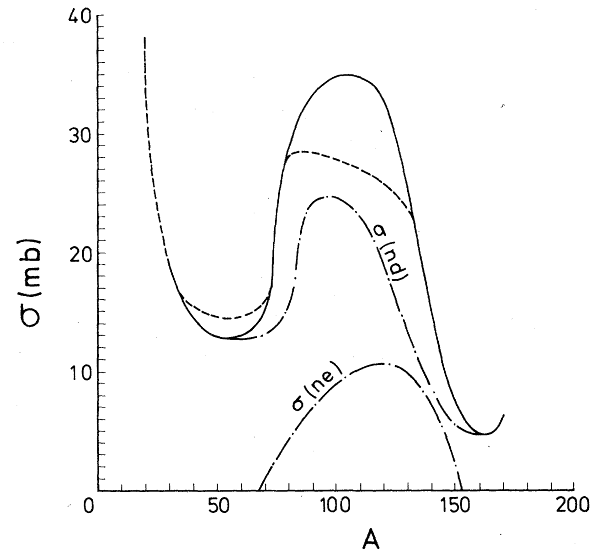

FIG. 2. Isobaric yield curve from the interaction of uranium with 11–29 GeV protons. The dashed line is taken from Ref. 5. The dot-dashed lines are the isobar yield curves of neutron-excessive and neutron-deficient products.

angular distribution of ^{131}Ba, the Purdue group explained that the products could be formed by a fragmentation process.[2,9] However, this process has not been fully specified at this time.

For further study of these yields, a nonlinear least square program has been used to decompose each CDC to fit the experimental points with the sum of two Gaussians in the following expression

$$\sigma(Z) = \sigma_{\max}(\text{ne}) \exp\{-[Z - Z_p(\text{ne})]^2/2S^2(\text{ne})\} + \sigma_{\max}(\text{nd}) \exp\{-[Z - Z_p(\text{nd})]^2/2S^2(\text{nd})\},$$

where (ne) refers to the neutron-excessive Gaussian and (nd) to the neutron-deficient one. The Gaussian parameters were obtained by a number of iterations and are summarized in Table III. The mass yield curve of neutron-deficient Gaussian and neutron-excessive Gaussian are plotted as dot-dashed curves shown in Fig. 2, where the solid curve in the figure represents the isobaric yield curve obtained by summing up each CDC. Since we have a few more CD curves reported recently, it makes the isobaric yield curve a little different from the one reported by Chu *et al.*[5] The solid curve (contrast the dashed curve) shows essentially a peak rather than a flat top in the region $A = 80$ and $A = 140$.

The results of these curves provide some interesting information about the two mechanisms. They show that the neutron-excessive products are produced in a narrow mass region between $A = 70$ and $A = 150$ and have a peak at half of the target mass, indicating that they could be formed through oscillation of the two nearly equal size fragments before splitting. With the recoil range data, these products known are formed through a binary fissionlike process.

On the other hand, the neutron-deficient products cover the entire mass region. The mass yield curve shows a peak at around $A = 90$, and a trend falling to a constant at $A \geq 150$, where $\sigma = 6$ mb. On the light fragments region the curve becomes flat at $A = 70$ to $A = 40$ and then rises sharply as A decreases. There are a number of mechanisms that have been suggested to yield these products such as: the shock wave approximation,[12] the double center oscillator process,[13] and the gluon multinuclear process,[14] etc. From the forward-to-backward recoil range ratio of ^{24}Na, ^{131}Ba, and $^{44}Sc^m$ which show a peak at 1–4 GeV,[15,2,9] we feel these yields are most likely formed through the creation and decay of a vector meson inside the target nuclide, causing the fast break of the target into two or more parts. That would induce yields

TABLE III. Charge-dispersion parameters.

A	47	72	87	111	131	147	170
$\sigma_{\max}$(nd)	6.3	5.8	7.4	2.6	2.96	2.54	2.78
Z_p(nd)	20.98	32.0	37.99	49.12	56.46	64.44	72.65
N/Z_p	1.24	1.25	1.29	1.26	1.32	1.27	1.34
FWHM	2.05	2.13	3.50	2.31	2.31	2.34	2.42
σ_{tot}(nd)	12.97	12.94	24.24	6.5	13.49	6.04	6.41
$\sigma_{\max}$(ne)		1.8	4.50	9.2	3.81	1.02	
Z_p(ne)		30.0	35.22	46.24	52.21	58.14	
N/Z_p		1.40	1.47	1.41	1.51		
FWHM		1.37	1.82	2.90	2.44	3.30	
σ_{tot}(ne)		2.6	8.10	28.5	9.88	3.58	
$\sum\sigma_{tot}$	12.97	15.54	32.34	35.00	23.37	9.62	6.41

characterized by fragmentation or deep spallation-like products.

The author wishes to thank Professor N. T. Porile for sending copies of the A_Z and Z_{eff} values of Chu, Starzyk, and Sugarman, and of Yu and Porile for use in the abscissa transformation of CD curves. He also expresses his appreciation to Professor F. C. Strong.

---

[1]G. Friedlander, *Physics and Chemistry of Fission* (IAEA, Vienna, 1965), Vol. II, p. 265.
[2]K. Beg and N. T. Porile, Phys. Rev. C 3, 1631 (1971).
[3]Y. W. Yu and N. T. Porile, Phys. Rev. C 7, 1597 (1973).
[4]Y. Y. Chu, G. Friedlander, and L. Husain, Phys. Rev. C 15, 352 (1977).
[5]Y. Y. Chu, E. M. Franz, G. Friedlander, and P. J. Karol, Phys. Rev. C 4, 2202 (1971).
[6]S. Kaufman, quoted in Ref. 1.
[7]J. A. Panontin and N. T. Porile, J. Inorg. Nucl. Chem. 32, 1775 (1970).
[8]J. Chanmont, Ph.D. thesis, University of Paris, 1970 (unpublished).
[9]O. Scheidemann and N. T. Porile, Phys. Rev. C 14, 1534 (1976).
[10]P. M. Starzyk and N. Sugarman, Phys. Rev. C 8, 1448 (1973).
[11]J. Hudis and S. Katcoff, Phys. Rev. 180, 1122 (1969).
[12]L. P. Remsberg and D. G. Perry, Phys. Rev. Lett. 35, 361 (1975).
[13]H. J. Fink, J. Maruhn, W. Scheid, and W. Greiner, Z. Phys. 228, 321 (1974).
[14]L. J. Gutay, report, 1978 (unpublished).
[15]S. B. Kaufman and M. W. Weisfield, Phys. Rev. C 11, 1259 (1975).